Dentomaxillofacial Radiology (2020) 49, 20190364

birpublications.org/dmfr

TECHNICAL REPORT

Validation of a 3D CBCT-based protocol for the follow-up of mandibular condyle remodeling

[1,2]Pieter-Jan Verhelst, [1,2]Eman Shaheen, [1]Karla de Faria Vasconcelos, [1,2]Fréderic Van der Cruyssen, [1]Sohaib Shujaat, [3]Walter Coudyzer, [4,5]Benjamin Salmon, [6]Gwen Swennen, [1,2]Constantinus Politis and [1,2,7]Reinhilde Jacobs

[1]OMFS IMPATH Research Group, Department of Imaging and Pathology, Faculty of Medicine, KU Leuven, Leuven, Belgium; [2]Department of Oral and Maxillofacial Surgery, University Hospitals Leuven, Leuven, Belgium; [3]Department of Radiology, University Hospitals Leuven, Leuven, Belgium; [4]Orofacial Pathologies, Imaging and Biotherapies EA2496 Lab, University of Paris, Montrouge, France; [5]Dental Medicine Department, AP-HP, Bretonneau Hospital, Paris, France; [6]Division of Maxillofacial Surgery, Department of Surgery, AZ Sint-Jan Brugge-Oostende AV, Bruges, Belgium; [7]Department of Dental Medicine, Karolinska Institutet, Stockholm, Sweden

Objectives: Three-dimensional models of mandibular condyles provide a way for condylar remodeling follow-up. The overall aim was to develop and validate a user-friendly workflow for cone beam CT (CBCT)-based semi-automatic condylar registration and segmentation.
Methods: A rigid voxel-based registration (VBR) technique for registration of two post-operative CBCT-scans was tested. Two modified mandibular rami, with or without gonial angle, were investigated as the volume of interest for registration. Inter- and intraoperator reproducibility of this technique was tested on 10 mandibular rami of orthognathic patients by means of intraclass correlation coefficients (ICC's) and descriptive statistics of the transformation values from the VBR. The difference in reproducibility between the two modified rami was evaluated using a paired *t*-test ($p < 0.05$). For the segmentation, eight fresh frozen cadaver heads were scanned with CBCT and micro-CT. These data were used to test the inter- and intraoperator reproducibility (ICC's) and accuracy (Bland–Altman plot) of a newly designed workflow based on semi-automated contour enhancement.
Results: Excellent ICC's (0.94–0.99) were obtained for the voxel-based registration technique using both modified rami. If the gonial angle was not included in the volume of interest, there was a trend of increased operator error suggested by significant higher interoperator differences in translation values ($p = 0{,}0036$). The segmentation workflow proved to be highly reproducible with excellent ICC's (0.99), low absolute mean volume differences between operators (23.19 mm^3), within operators (28.93 mm^3) and low surface distances between models of different operators (<0.20 mm). Regarding the accuracy, CBCT-models slightly overestimate the condylar volume compared to micro-CT.
Conclusions: This study provides a validated user-friendly and reproducible method of creating three-dimensional-surface models of mandibular condyles out of longitudinal CBCT-scans.
Dentomaxillofacial Radiology (2020) **49**, 20190364. doi: 10.1259/dmfr.20190364

Cite this article as: Verhelst P-J, Shaheen E, de Faria Vasconcelos K, Van der Cruyssen F, Shujaat S, Coudyzer W, et al. Validation of a 3D CBCT-based protocol for the follow-up of mandibular condyle remodeling. *Dentomaxillofac Radiol* 2020; **49**: 20190364.

Keywords: Mandibular condyle; Cone-Beam Computed Tomography; Three-Dimensional Imaging; Bone Remodeling; Orthognathic Surgery

Correspondence to: Dr Pieter-Jan Verhelst, E-mail: verhelst.pieterjan@gmail.com

Received 15 September 2019; revised 17 October 2019; accepted 25 October 2019

Objectives

The mandibular condyle is known to remodel in response to a change in position or function. This is frequently the case in orthognathic surgery.[1] Adaptive postoperative structural changes occur, leading to an altered shape of the condyle. In some cases, this adaptive process exceeds its limits and transgresses into pathological remodeling. A feared outcome of pathological remodeling is condylar resorption, characterized by excessive volume loss, reduction of the ramal height and posterior facial height with the emergence of an anterior open bite.[2,3]

Cone beam computed tomography (CBCT) has become a well-established imaging modality in oral and maxillofacial surgery and dental practices and a valuable tool to evaluate bone remodeling. This has led to the development of studies that are looking into remodeling and resorption using three-dimensional (3D) surface models of the condyle derived from CBCT-imaging. To be able to compare 3D surface models of follow-up CBCT-scans, the 3D-data sets need to be aligned and 3D surface models of the condyles need to be created in an accurate and reproducible way.[4]

The alignment of follow-up scans is most accurately performed by voxel-based registration (VBR).[5,6] Algorithms match voxels with the same grayscale values that are included in an operator-defined volume. Ideally, a volume of interest for registration is selected that has a stable position in relation to the mandibular condyle. However, the condylar segmentation based on CBCT-data remains challenging. Low bone density of the condyle, connected soft tissues, a close relationship with the glenoid fossa, conical shape of the CBCT beam, the high density petrous part of the temporal bone and an intrinsic low contrast resolution of the CBCT-data are hurdles for automated segmentation algorithms.[7]

Validation of VBR and segmentation techniques is crucial for a correct interpretation of results based on 3D model comparison evaluation. The aim of this study was to develop and validate a user-friendly workflow for CBCT-based semi-automatic condylar registration and segmentation allowing condylar remodeling follow-up and diagnose potential resorption.

Methods

The study protocol was approved by the ethical commission of the University Hospitals of Leuven, Leuven, Belgium (protocol number NH019-2018-03-02) and the study consisted of two parts. In the first part, the inter- and intraoperator reproducibility of a voxel-based registration technique using modified rami as a volume of interest for registration was tested (Figure 1). In the second part, the accuracy as well as the inter- and intraoperator reproducibility of the segmentation was assessed (Figure 2).

Part 1—image registration

Study data: For the VBR, 10 patients were randomly selected out of the LORTHOG-database containing data from a cohort observational study which evaluates patients having orthognathic surgery at the Department of Oral and Maxillofacial Surgery of the University Hospitals of Leuven. All selected patients had a bilateral sagittal split osteotomy of the mandible. These patients received a CBCT-scan for pre-operative evaluation and virtual surgery planning. Follow-up CBCT-scans were acquired for post-operative evaluation of the osteotomy sites, hard tissue remodeling and skeletal stability. CBCT-scans were obtained at the 1 week (1w) and 6 months (6m) follow-up visits according to the department's clinical practice protocol with the patients seated in the natural head positioning with a thin wax bite keeping them in centric relation. The Newtom VGi evo device (QR Verona, Verona, Italy) was used with the scanning parameters of field of view (FOV) 24 × 19 cm, voxel size 0.3 mm^3, 110 kVp and 4.3 mA. The DICOM files of these scans were extracted and anonymized. Registration was performed using the left ramus of each patient.

Registration method: To align the 6 m CBCT with the 1w CBCT, VBR was performed in the Amira software (v. 6.7.0, Thermo Fischer Scientific, Merignac, France). Both DICOM series were loaded in the software and a programmed wizard was used for the procedure. After importing the DICOM files, a common and stable volume of interest was delineated in both scans by the operator. This volume of interest was used to transform the 6 m CBCT-scan towards the 1w CBCT-scan, so the gray values of the voxels included in the volume of interest are matched. A modified ramus was delineated to serve as a volume of interest. Two types of modified rami were tested. Modified ramus 1 (MR1) consisted out of the coronoid process, the part of the ramus between the sigmoidal notch and the lingula and the adjacent posterior border of the ramus including the gonial angle. Modified ramus 2 (MR2) had the same configuration as MR1 except for the exclusion of the gonial angle. Operators delineated the volume of interest manually based on a volume render of the mandible. In both options, the condyle itself was excluded from the volume of interest using a user-defined cut-off plane going through the lowest point of the sigmoid notch and parallel to the lower border of the mandible. To compare the registrations between and within operators, the transformation matrix of each registration was extracted out of the Amira software according to a technique used by Shaheen et al in a previous validation study.[8] The rigid transformation consists out of translation values (displacement on the x-, y- and z-axis) as well as rotational values (displacement by pitch, roll, and yaw) that define the movement of the 6 m CBCT

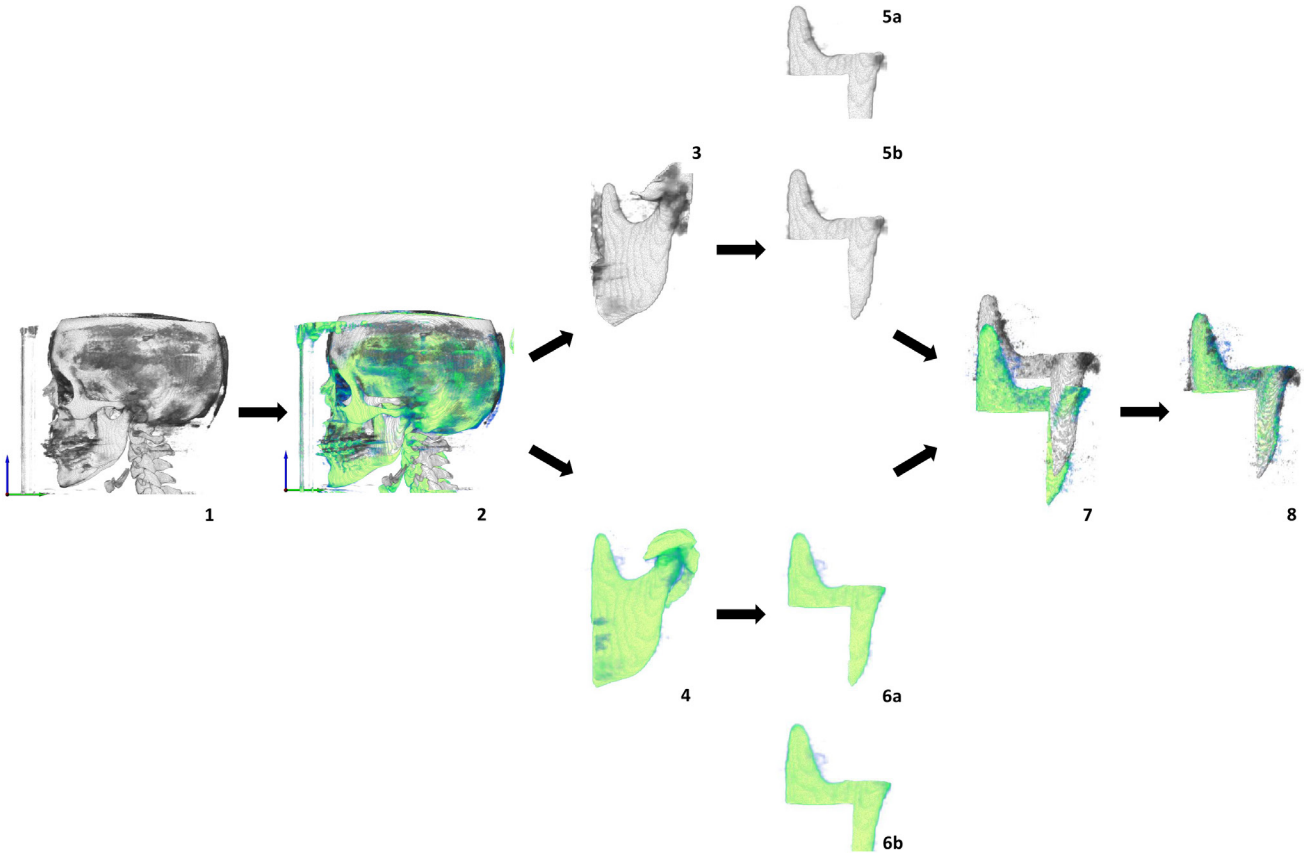

Figure 1 VBR workflow Illustration of the voxel-based registration workflow using a modified ramus in the Amira software. (**1**) The immediate post-operative CBCT-scan (gray) is loaded into the wizard. (**2**) The 6 months postoperative CBCT-scan (green) is loaded into the wizard. Both scans are clearly not aligned yet. (**3**) The left ramus is isolated out of the immediate post-operative CBCT-scan. (**4**) The same steps are followed for the 6 months post-operative CBCT-scan. (**5**) A modified ramus is created in the immediate post-operative CBCT-scan by isolating the coronoid, a part between sigmoid notch and split and the posterior border behind the split a) including the gonial angle and b) excluding the gonial angle. (**6**) The same steps are followed for the 6 months post-operative CBCT-scan. (**7**) Both modified rami before voxel-based registration. (**8**) Both modified rami after voxel-based registration. CBCT, cone beam CT; VBR, voxel-based registration.

scan to match the 1w CBCT scan. Ideally, these should be identical when repeated in the same patient

Registration validation: The voxel-based registration was performed on the 10 randomly selected patients independently by two operators after initial calibration on how to delineate the modified rami. The first operator performed the registration a second time after a 2-week interval. This was done for both MR1 as MR2. Data were analyzed using MedCalc statistical software (v. 12,0, Ostend, Belgium). A two-way model intraclass correlation coefficient (ICC) for absolute agreement was applied for assessing inter- and intraoperator agreement regarding the translation and rotational values of the transformation matrices. This was done for MR1 as well as MR2. The absolute mean and standard deviation were also calculated. Next, we evaluated if there was a difference in the reproducibility of the VBR using MR1 or MR2. A paired *t*-test was used to evaluated if the differences between and within operator transformation matrix values changed significantly when either MR1 or MR2 was used as volume of interest for registration. A *p*-value of <0.05 was regarded as statistically significant.

Part 2—segmentation

Study data: For the development and validation of the segmentation method, eight fresh frozen cadaver heads were obtained. All heads were scanned using the Newtom VGi evo CBCT with the scanning parameters of FOV 16 × 16 cm, voxel size 0.3 mm^3, 110 kVp and 5.4 mA. Evaluation of the scans identified two patients who have had a condylectomy. This resulted in 14 condyles available for testing. The mandibles were isolated out of the fresh frozen cadaver heads by dissection and were then cleaned by submerging them for 2 h in water of 80°C and removal of the remaining soft tissue manually. Afterward, the mandibular rami, including the condyles were cut out of the mandibular body and were scanned by micro-CT (MCT) device Quantum FX Caliper (Life Sciences, Perkin Elmer, Waltham, MA) using scanning parameters FOV 4 × 4 cm, voxel size 0.08 mm^3, 90 kV,

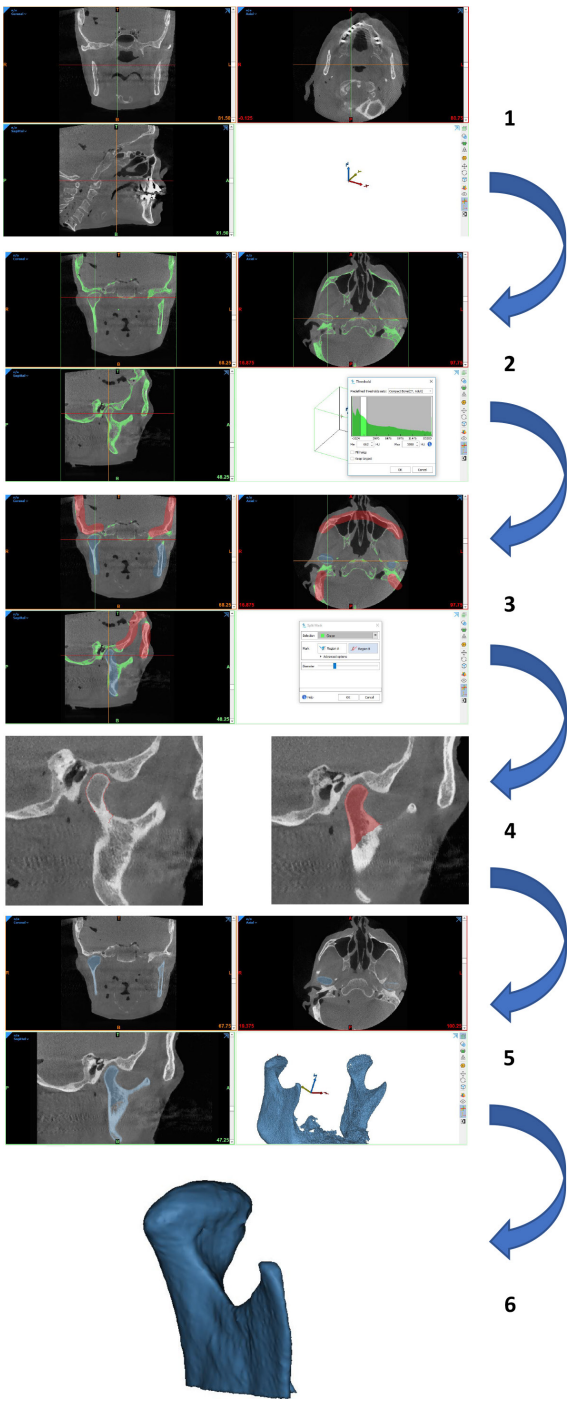

Figure 2 Segmentation workflow Illustration of the segmentation workflow in the Materialise Mimics software. (**1**) The CBCT-scan is loaded into the software suite and visualized. (**2**) Thresholding using the compact bone range is performed to create a rough first 3D-model. Especially in the condylar region, regions of cortical bone are not included, and the 3D-model is incomplete. (**3**) The mandible is isolated out of the 3D model (blue) by splitting the initial model. (**4**) The condyle is enhanced by using the livewire tool. Automatic contour recognition is performed every five slices in the sagittal view. The contour in between is interpolated. (**5**) The resulting enhanced 3D model is checked for inaccuracies and corrected if necessary. (**6**) The condyle is isolated out of the model and is ready for analysis. 3D, three-dimensional; CBCT, cone beam CT.

160 μA, 120 s, 360° of rotation, and a 0.1 mm aluminium filter). The MCT representation of the condyle was regarded as anatomical reality regarding bony tissue due to the high resolution and absence of soft tissues.

Segmentation method: The DICOM files of the CBCT-scans of the fresh frozen cadaver heads were loaded in the Mimics software (v. 21.0, Materialise, Leuven, Belgium). A semi-automated segmentation workflow was used. First, classic thresholding was applied using the preset adult compact bone CT interval to obtain a rough segmentation of the complete skull. Subsequently, the created mask was split into a mandibular part and a skull part. The mandibular mask was isolated, and the condyles were enhanced. This was performed using the multislice livewire edit tool available in the software. Using this tool, the cursor is attracted in between pixels with a high variation of gray value, in this case, the cortical bone of the condyle and its surrounding soft tissues. The sagittal slice containing the last visible part of the lateral pole of each condyle was identified and a contour was semi-automatically delineated by hovering over the cortical contour of the condyle whilst the software fitted a contour line. For every five slices, the contour was created, and the software interpolated it for the slices in between. This was performed for the condylar head and neck, as this region contained most inaccuracies (holes in the segmentation mask) produced by thresholding. Afterward, the surface model was checked for under- and overcontouring and was corrected whenever necessary. Performing this procedure for one skull with two condyles took between 15 and 20 min.

Segmentation validation: To assess reproducibility of the method, two operators created surface models of all cadaver condyles out of the CBCT-scans using the aforementioned method (P1 & F1). The first operator did this twice with a 2-week interval (P1 & P2). All surface models of a given condyle (P1, P2, F1) were subsequently loaded into the 3D analytical and design software 3-Matic (v. 13.0, Materialise, Leuven, Belgium). Since every operator worked on the same DICOM data, surface models should overlap and differences in the surface could be regarded as operator differences. The caudal border of all condyles was determined by an analytical sphere, created in 3-Matic, as performed by Nicolielo et al in a previous study on this topic.[9] To create this analytical sphere, the superior pole of the P1 condyle served as a midpoint and the radius was set to 20 cm. Volumes of the resulting condyles were calculated. Next, closest point distance mapping between the surfaces was performed. The root mean square (RMS) distance was calculated as it gives information on the absolute mean distance between the surfaces. Minimum and maximum distances between surfaces were also extracted. This was done for the complete surface and for four defined sectors of the condyle (S1, S2, S3, S4). These sectors were created by dividing the condyles by

a plane through the lateral and medial pole of the P1 condyle parallel through the horizontal reference plane and a midplane perpendicular on this first plane.
For accuracy evaluation, MCT-scans of the isolated rami were aligned with their respective CBCT-scans. Next, 3D surface models were constructed out of the MCT-data using mere thresholding. These served as the golden standard. The P1 models were compared with the MCT models by evaluating volumes and closest point distance mapping between surfaces.

All data were analyzed using MedCalc Statistical software (v. 12.0, Ostend, Belgium). For the evaluation of the reproducibility, a two-way model intraclass correlation coefficient (ICC) for absolute agreement was applied for assessing inter- and intraoperator agreement of the volumes. Descriptive statistics were calculated for the RMS, minimum and maximum distances between surfaces of all 14 condyles created by the operators. For the evaluation of the accuracy, a Bland–Altman plot was used to compare the interchangeability of the two methods based on volume. Descriptive statistics were also calculated for the RMS.

Results

Registration
Two volumes of interest (MR1 and MR2) were evaluated for reproducibility of the registration procedure. Table 1 illustrates the results of the inter- and intraoperator agreement using ICC for translational and rotational movements performed during the registration procedure for both MR1 as MR2. Excellent ICC's were obtained ranging from 0.94 to 0.99. Absolute mean differences between and within operators remained well below 1 mm for translation and 1.2° for rotation. As for the difference in reproducibility between the MR1 and the MR2, a slightly higher interoperator absolute mean difference in translation was noted in the MR2 group, which could imply a higher risk for interoperator error when not including the gonial angle in the volume of interest. Paired *t*-tests confirmed this difference to be statistically significant ($p = 0.0036$). The remaining differences between MR1 and MR2 were not statistically significant (Table 2).

Segmentation
Table 3 gives an overview of the results of the inter- and intraoperator reproducibility of the segmentation. Excellent ICC's of 0.99 were obtained with mean absolute volume differences of less than 30 mm^3. Table 4 provides an overview of the mean distances between the surfaces of the different operator models. The RMS provides an absolute mean distance between the complete surfaces of two models. For the complete condyles, intra- and interoperator absolute distances between surfaces were very low (0.13 mm). The RMS of the respective sectors of the condyle were all below 0.20 mm.

Figure 3 is the graphic representation of the Bland–Altman plot used to evaluate the accuracy of the segmentation method, based on the resulting volumes. The P1-models were compared to the MCT models and the latter were regarded as the golden standard. The graph illustrates that the CBCT models overestimate the golden standard with a mean of 1.9 mm^3. The limits of agreement were found to be +64.0 and −67.7 mm^3. This means CBCT and MCT results can be regarded as interchangeable when an absolute mean error of 67.7 mm^3 is accepted. The absolute mean distance between the complete surfaces of the MCT models and the P1 models was 0.17 mm.

Discussion

This study validated a new registration and segmentation workflow for creating 3D surface models of mandibular condyles out of CBCT-data. Creating 3D surface models of mandibular condyles in an accurate and reproducible way is a prerequisite for further analysis and diagnosis of remodeling and resorption of the condyle. Volume analysis can be performed above a reproducible cut-off plane such as the C-plane defined by Xi et al.[10] Shape analysis methods such as the slicerSALT project (salt.slicer.org, Victory et al 2018) use methods to identify anatomical correspondent points. These points can then be used to quantify the amount and direction of remodeling of the cortical contour.

Previous studies evaluating condylar remodeling often used the cranial base as a volume of interest for VBR.[11–13] From a biomechanical viewpoint, this

Table 1 Intra- and inter operator voxel-based registration reproducibility

	Translation		*Rotation*	
	ICC	*Mean AD ±SD (mm)*	*ICC*	*Mean AD ±SD (°)*
Intraoperator MR1	0,99	0,49 ± 0,56	0,96	0,95 ± 0,81
Interoperator MR1	0,99	0,26 ± 0,28	0,96	0,74 ± 1,06
Intraoperator MR2	0,99	0,31 ± 0,22	0,94	1,03 ± 1,09
Interoperator MR2	0,99	0,68 ± 0,78	0,94	1,16 ± 1,03

AD, absolute difference; *ICC*, interclass correlation coefficient; MR1, modified ramus with gonial angle; *MR2*, modified ramus without gonial angle; *SD*, standard deviation.

Table 2 Differences between MR1 and MR2 reproducibility

	Translation		*Rotation*	
	Mean Δ ± SD (mm)	p-*value*	*Mean Δ ± SD (°)*	p-*value*
Intraoperator MR1 *vs* MR2	−0,18 ± 0,53	0,0759	0,09 ± 1,23	0,7033
Interoperator MR1 *vs* MR2	0,42 ± 0,73	0,0036*	0,41 ± 1,19	0,0667

Δ, difference; *MR1*, modified ramus with gonial angle; *MR2*, modified ramus without gonial angle; *SD*, standard deviation.
* statistically significant

technique is hypothetically incorrect. The mandible articulates with the skull base through its TMJ. This means that the position of the condyle in the joint depends on mouth opening, occlusion, use of a wax bite in centric relation or maximal occlusion, morphological changes of the condyle or displacement caused by surgery. These variables make it impossible to distinguish condylar remodeling from condylar displacement when using the skull base as a volume of interest for VBR.

The present study opted for a part of the mandible as a volume of interest that was believed to be dimensionally stable in relation to the condyle that is investigated. It included the coronoid process, the ramal part between the sigmoid notch and the posterior border of the ramus. A version with and without gonial angle was evaluated and both proved highly reproducible regardless of the operator. Slightly higher absolute mean differences for translation and rotation values within and between operators were obtained in the modified ramus without a gonial angle with only the difference in inter operator translation being significantly higher. This can be due to the fact that the caudal cut-off of the volume of interest had to be identified manually by operators.

When DICOM-data have been transformed by VBR, segmentation techniques deliver the actual 3D surface models. Mere thresholding is mostly insufficient in delivering a complete cortical outline of the condyle due to low bone density of the condyle, connected soft tissues, a close relationship with the glenoid fossa, conical shape of the CBCT beam, the high density petrous part of the temporal bone and an intrinsic low contrast resolution of the CBCT-data.[7] Different semi-automated region-growing segmentation techniques have been presented in the literature.[14,15] One of the downsides of region-growing techniques is that due to the low contrast in this region, the segmentation result often includes bridges between condyle and fossa that are anatomically non-existent. Even if an "automated" protocol is used, post-processing and corrections are obligatory. The presented technique followed a reversed approach to cancel out these corrections. A base condyle was obtained by thresholding and was then augmented using a semi-automated contour recognition tool. This was done in a commercially available and user-friendly software package that is intuitive to use for clinicians. Inter- and intraoperator differences in volumes were in line with or lower than other studies using semi-automated region-growing techniques.[9,15] The technique was therefore deemed reproducible for acquiring 3D surface models in a consistent way.

The advantage of using fresh frozen cadaver heads for this study was the option to compare the clinical 3D models with anatomical reality. After the CBCT-acquisition, the mandible could be isolated out of the remaining tissue and used as a golden standard by scanning it with micro-CT. The small voxel size of micro-CT makes highly accurate 3D reconstructions possible.[16,17] The results show that CBCT-derived 3D-models of the condyle slightly overestimate the volume of the actual condyle. Based on this finding, statements that put emphasis on the actual volume of a condyle should be interpreted with caution. However, when condyles are

Table 3 Intra- and interoperator segmentation reproducibility based on condylar volumes

	ICC	*Mean AD ±SD (mm³)*
Intraoperator	0,99	28,93 ± 15,9
Interoperator	0,99	23,19 ± 22,3

AD, absolute difference; ICC, interclass correlation coefficient; *SD*, standard deviation.

Table 4 Mean (n = 14) surface distances between operator models

		Mean intraoperator (mm)	*Mean interoperator (mm)*
Complete	RMS	0,13 ± 0,04	0,13 ± 0,05
	Min	−0,54 ± 0,36	−0,60 ± 0,47
	Max	0,56 ± 0,16	0,58 ± 0,19
S1	RMS	0,13 ± 0,05	0,13 ± 0,04
	Min	−0,33 ± 0,29	−0,35 ± 0,23
	Max	0,43 ± 0,13	0,45 ± 0,14
S2	RMS	0,17 ± 0,06	0,17 ± 0,08
	Min	−0,38 ± 0,29	−0,43 ± 0,45
	Max	0,49 ± 0,14	0,51 ± 0,17
S3	RMS	0,09 ± 0,04	0,1 ± 0,05
	Min	−0,27 ± 0,12	−0,30 ± 0,1
	Max	0,42 ± 0,14	0,46 ± 0,22
S4	RMS	0,12 ± 0,03	0,12 ± 0,05
	Min	−0,38 ± 0,21	−0,36 ± 0,20
	Max	0,51 ± 0,13	0,47 ± 0,15

Complete, complete condyle; Max, maximal distance between surfaces; Min, minimal distance between surfaces;RMS, Root mean square distance between surfaces; S1, upper lateral sector; S2, upper medial sector; S3, lower lateral sector; S4, lower medial sector.

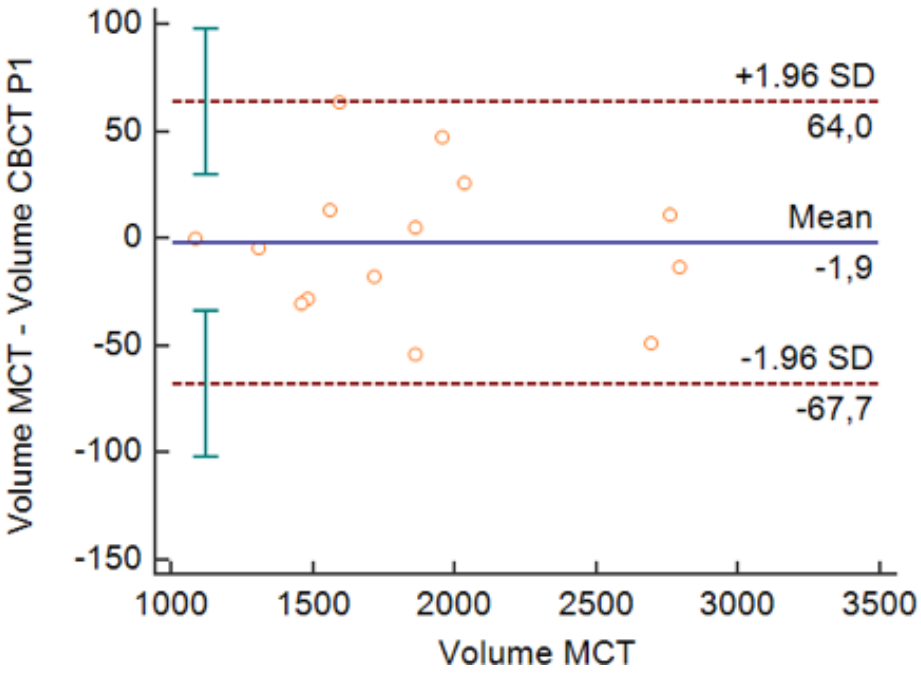

Figure 3 Accuracy of the segmentation based on volumes. Bland–Altman plot for evaluation of the agreement between the volume of the condyles of the CBCT-models and the MCT-models. There is no trend in bigger difference between methods if the condylar volume increases. CBCT overestimates MCT with a mean of 1.9 mm^3. CBCT and MCT can be regarded as equivalent if an error of 67.7 mm^3 is accepted. CBCT, cone beam CT; MCT, micro-CT.

segmented with a reliable technique, it is safe to assume the error will always be present in the segmentation. In this way, by comparing the change of volume in two longitudinal scans of the same patient, the mean overestimation will be canceled out.

This study did have some limitations. Registration and segmentation were carried out in two separate commercial software packages. They offered the advantage of powerful and intuitive workflows but have the downside requiring a license at a financial cost and interrupting your workflow when switching between programs. The registered data sets always needed to be manually imported in the segmentation software. Next, the VBR using the modified ramus was developed in patients who had an Obwegeser-Dalpont split of the ramus with a Hunsuck modification. This means the posterior border is unaffected by the split and can be regarded as a possible volume of interest for registration. However, further studies are needed to confirm the hypothesis that the posterior border of the ramus does not remodel following surgery. Also, if other types of sagittal split ramus osteotomies are used, the volume of interest selection for VBR needs to be readdressed. Last, the segmentation workflow remains a semi-automated approach, requiring operator input. This will always introduce some error and needs to be kept in mind when interpreting the results of patient analysis studies.

Conclusion

This study illustrated a reliable way of creating 3D surface models of the mandibular condyle for patient follow-up using voxel-based registration based on a modified ramus and a semi-automated segmentation workflow based on contour recognition. CBCT-derived 3D-models using this technique mildly overestimate the real condylar volume but can be used for evaluating volumetric change. These 3D-models can serve for analysis techniques like volumetric analysis and shape analysis.

References

1. Arnett GW, Gunson MJ. Risk factors in the initiation of condylar resorption. *Semin Orthod* 2013; **19**: 81–8. doi: https://doi.org/10.1053/j.sodo.2012.11.001
2. Hoppenreijs TJM, Maal T, Xi T. Evaluation of condylar resorption before and after Orthognathic surgery. *Semin Orthod* 2013; **19**: 106–15. doi: https://doi.org/10.1053/j.sodo.2012.11.006
3. Politis C, Van De Vyvere G, Agbaje JO. Condylar resorption after Orthognathic surgery. *J Craniofac Surg* 2019; **30**: 169–74. doi: https://doi.org/10.1097/SCS.0000000000004837
4. Verhelst PJ, Verstraete L, Shaheen E, Shujaat S, Darche V, Jacobs R, et al. Three-Dimensional cone beam computed tomography analysis protocols for condylar remodelling following orthognathic surgery: a systematic review. *Int J Oral Maxillofac*

Surg 2019;epub ahead of print. doi: https://doi.org/10.1016/j.ijom.2019.05.009
5. Almukhtar A, Ju X, Khambay B, McDonald J, Ayoub A. Comparison of the accuracy of voxel based registration and surface based registration for 3D assessment of surgical change following orthognathic surgery. *PLoS One* 2014; **9**: e93402. doi: https://doi.org/10.1371/journal.pone.0093402
6. Nada RM, Maal TJJ, Breuning KH, Bergé SJ, Mostafa YA, Kuijpers-Jagtman AM. Accuracy and reproducibility of Voxel based superimposition of cone beam computed tomography models on the anterior cranial base and the Zygomatic Arches. *PLoS One* 2011; **6**: e16520. doi: https://doi.org/10.1371/journal.pone.0016520
7. Engelbrecht WP, Fourie Z, Damstra J, Gerrits PO, Ren Y. The influence of the segmentation process on 3D measurements from cone beam computed tomography-derived surface models. *Clin Oral Investig* 2013; **17**: 1919–27. doi: https://doi.org/10.1007/s00784-012-0881-3
8. Shaheen E, Shujaat S, Saeed T, Jacobs R, Politis C. Three-Dimensional planning accuracy and follow-up protocol in orthognathic surgery: a validation study. *Int J Oral Maxillofac Surg* 2019; **48**: 71–6. doi: https://doi.org/10.1016/j.ijom.2018.07.011
9. Nicolielo LFP, Van Dessel J, Shaheen E, Letelier C, Codari M, Politis C, et al. Validation of a novel imaging approach using multi-slice CT and cone-beam CT to follow-up on condylar remodeling after bimaxillary surgery. *Int J Oral Sci* 2017; **14**: 1–6.
10. Xi T, Schreurs R, van Loon B, de Koning M, Bergé S, Hoppenreijs T, et al. 3D analysis of condylar remodelling and skeletal relapse following bilateral sagittal split advancement osteotomies. *Journal of Cranio-Maxillofacial Surgery* 2015; **43**: 462–8. doi: https://doi.org/10.1016/j.jcms.2015.02.006
11. de Paula LK, Ruellas ACO, Paniagua B, Styner M, Turvey T, Zhu H, et al. One-Year assessment of surgical outcomes in class III patients using cone beam computed tomography. *Int J Oral Maxillofac Surg* 2013; **42**: 780–9. doi: https://doi.org/10.1016/j.ijom.2013.01.002
12. Xi T, de Koning M, Bergé S, Hoppenreijs T, Maal T. The role of mandibular proximal segment rotations on skeletal relapse and condylar remodelling following bilateral sagittal split advancement osteotomies. *Journal of Cranio-Maxillofacial Surgery* 2015; **43**: 1716–22. doi: https://doi.org/10.1016/j.jcms.2015.07.022
13. Franco AA, Cevidanes LHS, Phillips C, Rossouw PE, Turvey TA, Carvalho FdeAR, et al. Long-Term 3-dimensional stability of mandibular advancement surgery. *Journal of Oral and Maxillofacial Surgery* 2013; **71**: 1588–97. doi: https://doi.org/10.1016/j.joms.2013.04.006
14. da Silva RJ, Souza GA, Ambrosano GMB, Freitas DQ, Freitas DQ, Sant'Ana E, et al. Changes in condylar volume and joint spaces after orthognathic surgery. *Int J Oral Maxillofac Surg* 2018; **47**: 511–7. doi: https://doi.org/10.1016/j.ijom.2017.10.012
15. Xi T, Schreurs R, Heerink WJ, Bergé SJ, Maal TJJ. A novel region-growing based semi-automatic segmentation protocol for three-dimensional condylar reconstruction using cone beam computed tomography (CBCT. *PLoS One* 2014; **9**: e111126. doi: https://doi.org/10.1371/journal.pone.0111126
16. Maret D, Telmon N, Peters OA, Lepage B, Treil J, Inglèse JM, et al. Effect of voxel size on the accuracy of 3D reconstructions with cone beam CT. *Dentomaxillofac Radiol* 2012; **41**: 649–55. doi: https://doi.org/10.1259/dmfr/81804525
17. Pauwels R, Faruangsaeng T, Charoenkarn T, Ngonphloy N, Panmekiate S. Effect of exposure parameters and voxel size on bone structure analysis in CBCT. *Dentomaxillofac Radiol* 2015; **44**: 20150078.. doi: https://doi.org/10.1259/dmfr.20150078